ELSEVIER

International Journal of Pharmaceutics 221 (2001) 143–152

international journal of pharmaceutics

www.elsevier.com/locate/ijpharm

Effect of dose on the biodistribution and pharmacokinetics of PLGA and PLGA–mPEG nanoparticles

Z. Panagi [a], A. Beletsi [a], Gregory Evangelatos [b], E. Livaniou [b], D.S. Ithakissios [a], K. Avgoustakis [a,*]

[a] *Pharmaceutical Technology Laboratory, Department of Pharmacy, University of Patras, Rion 26500, Patras, Greece*
[b] *Institute of Radioisotopes and Radiodiagnostic Products, NCSR «Demokritos», Aghia Paraskevi Attikis, Athens 153 10, Greece*

Received 9 September 2000; received in revised form 23 March 2001; accepted 30 March 2001

Abstract

The effect of nanoparticle dose on the biodistribution and pharmacokinetics of conventional PLGA and stealth poly(Lactide-co-glycolide)–monomethoxypoly(ethyleneglycol) (PLGA–mPEG) nanoparticles was investigated. The precipitation-solvent diffusion method was used to prepare PLGA and PLGA–mPEG nanoparticles labeled with ^{125}I-cholesterylaniline. These were administered intravenously (i.v.) in mice and at predetermined time intervals the animals were sacrificed and their tissues were excised and assayed for radioactivity. Within the dose range applied in this study, blood clearance and mononuclear phagocyte system (MPS) uptake of the PLGA nanoparticles depended on dose whereas they were independent of dose in the case of the PLGA–mPEG nanoparticles. Increasing the dose, decreased the rates of blood clearance and MPS uptake of the PLGA nanoparticles, indicating a certain degree of MPS saturation at higher doses of PLGA nanoparticles. The dose affected the distribution of PLGA nanoparticles between blood and MPS (liver) but it did not affect the nanoparticle levels in the other tissues. Within the range of doses applied here, the PLGA nanoparticles followed non-linear and dose-dependent pharmacokinetics whereas the PLGA–mPEG nanoparticles followed linear and dose-independent pharmacokinetics. In addition to the prolonged blood residence, the dosage-independence of the pharmacokinetics of the PLGA–mPEG nanoparticles would provide further advantages for their application in controlled drug delivery and in drug targeting.

Keywords: poly(Lactide-co-glycolide); poly(Lactide-co-glycolide)-monomethoxy(polyethyleneglycol); Biodistribution; Pharmacokinetics; Effect of dose

1. Introduction

It has been long recognized that the efficient use of drugs requires that they should be delivered selectively at the site of action, preferably at a controlled rate. This is especially true for potent drugs with strong side effects, such as the anti-

* Corresponding author. Tel.: +30-61-997726; fax: +30-61-996302.
E-mail address: avgoust@patreas.upatras.gr (K. Avgoustakis).

0378-5173/01/$ - see front matter
PII: S0378-5173(01)00676-7

cancer drugs. In addition to selectivity, the delivery of the new generation of bioactive agents, such as proteins and genes, requires that they should be protected from in vivo inactivation before reaching their intracellular site of action. Polymeric nanoparticles, bearing or not a targeting moiety on the surface, are being investigated as intravenous (i.v.) drug carriers which when optimized might meet, to a large extent, the aforementioned drug delivery requirements (Couvreur et al., 1995; Kwon, 1998).

Between the different types of polymeric nanoparticles available, those currently receiving increased attention are the nanoparticles prepared from diblock poly(lactide)–monomethoxypoly(ethyleneglycol) (PLA–mPEG) and poly(lactide-co-glycolide)–monomethoxypoly(ethyleneglycol) (PLGA–mPEG) copolymers or from blends of these copolymers with PLA poly(Lactide) or PLGA poly(lactide-co-glycolide) (Gref et al., 1994; Stolnik et al., 1994; Bazile et al., 1995; Gref et al., 1995). PLA–mPEG and PLGA–mPEG nanoparticles combine a number of desirable, important characteristics for application in controlled drug delivery and in drug targeting, such as biocompatibility and biodegradability (Gref et al., 1994), persistence in blood following i.v. administration (Gref et al., 1994; Stolnik et al., 1994; Bazile et al., 1995), good encapsulation properties for lipophilic drugs (Gref et al., 1994; Peracchia et al., 1997) and neutral oligonucleotide complexes (Emile et al., 1996), and ability to be stored as freeze-dried powders until use, provided that appropriate freeze-drying conditions are employed (De Jaeghere et al., 1999; Zambaux et al., 1999).

So far, published information on the biodistribution of PLA–mPEG and PLGA–mPEG nanoparticles has concentrated mainly on their blood persistence and mononuclear phagocyte system (MPS) avoidance properties (Gref et al., 1994; Stolnik et al., 1994; Bazile et al., 1995). In the present study, the effect of nanoparticle dose on the tissue distribution and on the pharmacokinetics of PLGA and PLGA–mPEG nanoparticles administered i.v. in mice was investigated. The results reported could be useful to the rational design of PLGA–mPEG drug delivery systems with appropriate nanoparticle compositions, doses and dosing intervals, so as to maximize drug efficacy and minimize host defense impairment due to nanoparticle accumulation in MPS tissues.

2. Materials and methods

2.1. Materials

DL-lactide (LE) and glycolide (GE) were purchased from Boehringer Ingelheim (Germany). They were recrystallized twice from ethyl acetate and dried under high vacuum at room temperature before use. Monomethoxypoly(ethyleneglycol) (mPEG, molecular weight 5000) was obtained from Sigma (St. Louis, MO) and dried under high vacuum at room temperature before use. Stannous octoate, sodium cholate and cholesterylaniline (5-cholesten-3β-[*N*-phenyl]amine) were also obtained from Sigma. Sepharose CL-4B gel was purchased from Pharmacia (Sweden) and Biogel A15m from BIO-RAD. Tetrahydrofuran of HPLC grade and miscellaneous chemical reagents and solvents, all of analytical grade, were obtained from Sigma, Merck (Germany) and SDS (France). The $Na^{125}I$ was provided by NCSR 'Demokritos' (Greece) (source: MDS Nordion, Belgium).

2.2. Methods

2.2.1. Preparation and characterization of PLGA and PLGA–mPEG copolymers

Poly(lactide-co-glycolide) (PLGA) and poly(lactide-co-glycolide)–monomethoxy(polyethyleneglycol) (PLGA–mPEG) copolymers were prepared by a melt polymerization process under vacuum using stannous octoate as catalyst (Beletsi et al., 1999). They were characterized with regard to their composition by ^{1}H-NMR and their molecular weight and molecular weight distribution by gel permeation chromatography (GPC) (Beletsi et al., 1999). Two copolymers were used in this study; (a) PLGA with molar composition LA:GA = 2.8, $M_w = 22 \times 10^3$, and polydispersity index P.I. = $M_w/M_n = 1.9$ and (b) PLGA(32)–

mPEG(5) with composition LA:GA:EO = 4.0:1.7:1.0, $M_w = 37 \times 10^3$, and P.I. = 1.8. LA, GA and EO stand for lactic acid, glycolic acid, and ethyleneoxide components, respectively. The number in parenthesis following each block in the word PLGA–mPEG designates the molecular weight in kDa of the respective block, e.g. the PLGA(32)–mPEG(5) copolymer consists of a PLGA block with molecular weight 32 kDa plus a mPEG block with molecular weight 5 kDa (the molecular weight and the polydispersity index of the mPEG used were measured by GPC to be $M_w = 5200$ and P.I. = 1.1, respectively).

2.2.2. Preparation of ^{125}I-CA label

The ^{125}I was bound to cholesterylaniline (CA) using the iodine monochloride (ICl) method (New, 1990). The method requires the preparation of three solutions; (a) 2.5 mg/ml CA in $CHCl_3$/CH_3OH (1:1 v/v) (solution A), (b) 0.3 M NH_4Cl/NH_4OH in water (solution B) and (c) 2.5 mM ICl in water (solution C). An aliquot of Na^{125}I (10 μl, 4.1 mCi) was transferred in 40 μl of B and the mixture was heated at 44°C. Part (10 μl) of this mixture was transferred into a glass vial containing 200 μl of A and then 10 μl of C were added. After vortexing, the mixture was kept at room temperature for 1 h. The ^{125}I-CA formed was separated from the non-reacted ^{125}I by extraction of the reaction mixture in 1.2 ml of a 2/1 v/v $CHCl_3$/saline system. The ^{125}I-CA was collected in the $CHCl_3$ layer whereas ^{125}I passed in the aqueous phase. The solution of ^{125}I-CA in $CHCl_3$ was stored at 4°C until use. The labeling efficiency was checked by thin layer chromatography using a $CHCl_3$/CH_3OH/H_2O (65:25:4 by volume) mixture as eluent and was always higher than 95%.

2.2.3. Preparation of ^{125}I-CA-labeled PLGA and PLGA–mPEG nanoparticles

The precipitation-solvent diffusion method (Bazile et al., 1995) was applied to prepare ^{125}I-CA-labeled PLGA and PLGA–mPEG nanoparticles. The polymer and the label were dissolved in acetone and the solution was transferred dropwise into a stirred solution of sodium cholate (12 mM) in phosphate buffered saline (PBS, pH 7.4). Under these conditions the hydrophobic label was entrapped in the nanoparticles formed. The nanoparticle suspension was kept stirred until all acetone had been evaporated and then it was carefully condensed in a rotary evaporator (Buchi R114). Sodium cholate was used in the preparation of the nanoparticles because it has been found very effective in reducing the size and size range of the nanoparticles and because only a low amount of this surfactant remained associated with the nanoparticles after their preparation (Gref et al., 1995).

The non-entrapped label was removed by passing the nanoparticle suspension through a Sepharose CL-4B column (0.5 × 31 cm). The labeled nanoparticles were eluted using PBS as eluent and then the eluent was changed in a stepwise fashion from PBS to ethanol to elute the non-entrapped label (the label is soluble in ethanol). The labeling efficiency exceeded 70%. The solids concentration (μg of polymer per ml) in the labeled nanoparticle preparations (and thus the nanoparticle dose administered to the animals in the biodistribution studies) was calculated from the quantity of polymer added initially for the preparation of the nanoparticles taking into account the solids retention and the dilution of nanoparticles in the column.

The size and zeta potential of the nanoparticles employed in the study were determined using photon correlation spectroscopy (PCS) and microelectrophoresis, respectively, in a Malvern Z-sizer 5000 instrument (five runs per sample). The morphology of freeze-dried nanoparticle samples was examined using scanning electron microscopy (JEOL JSM-6300, Japan).

2.2.4. Stability of nanoparticle labeling in vitro

The stability of nanoparticle labeling with ^{125}I-CA was investigated by measuring the radioactivity remaining associated with the nanoparticles after incubation with mice serum in vitro. A 500 μl sample of purified, labeled nanoparticles (3.6 mg polymer per ml) was incubated with 500 μl mice serum for 6 h at 37°C. Another sample of the same nanoparticles was incubated under identical conditions in phosphate buffered saline serving as control. Then, the samples were loaded on a Biogel A15m column (1 × 45 cm) and the ra-

dioactivity eluted in the nanoparticle fractions, identified by eluent turbidity measurements, was measured. The stability of nanoparticle labeling was evaluated by comparing the radioactivity remaining on the nanoparticles, (i.e. the radioactivity eluted in the nanoparticle fractions) after their incubation in mice serum with the radioactivity remaining on the control nanoparticles.

2.2.5. Biodistribution studies

The tissue distribution of the ^{125}I-CA-labeled PLGA and PLGA–mPEG nanoparticles was determined in female Swiss-De mice weighing 25–30 g as described earlier (Allen, 1988; Chiotelis et al., 1977). The animals, three per group, were injected at random in the tail vein with 100–200 μl of a nanoparticle suspension containing the specified dose of nanoparticles (μg polymer per mouse) and at predetermined time intervals, covering a period of 10–60 s and 0.03–24 h for the PLGA and PLGA–mPEG nanoparticles, respectively, the mice were sacrificed and their tissues were excised, washed quickly with cold water to remove surface blood and counted for radioactivity. Blood samples (0.07–0.08 g) were obtained in duplicate by cardiac puncture in pre-weighed heparinized tubes. The percentage dose per organ was calculated taking that the blood, the bone and the muscle constitute 7, 10 and 43% of the body weight, respectively, (Chiotelis et al., 1977). The mice blood specific gravity was measured to be 1.083 g/ml. The biodistribution experiments adhered to the 'Principles of Laboratory Animal Care' (NIH publication # 85-23, revised 1985). The average ($n = 3$) blood radioactivity concentration versus time profiles obtained with each nanoparticle dose were analyzed to generate estimates for the basic pharmacokinetic parameters of the ^{125}I-CA-labeled PLGA and PLGA–mPEG nanoparticles.

3. Results

3.1. Nanoparticle characteristics

The nanoparticles prepared in this study appeared to be spherical under the scanning electron microscope (Fig. 1). The size and zeta potential (in PBS, pH 7.4) of the PLGA nanoparticles were 154.1 ± 23.5 nm (polydispersity 0.489) and -45.1 ± 1.9 mV, respectively, and of the PLGA(32)–mPEG(5) nanoparticles 113.5 ± 14.3 nm (polydispersity 0.385) and -3.9 ± 1.4 mV, respectively.

3.2. In vitro stability of labeling

The elution profiles of ^{125}I-CA-labeled PLGA(32)–mPEG(5) nanoparticles from the Biogel A15m column, after incubation in mice serum and in phosphate buffered saline (control), are shown in Fig. 2 (the results have been normalized in order the total radioactivity eluted from the column to be the same in both cases). Similar elution profiles were observed with the PLGA nanoparticles. In the case of the control nanoparticles, a major radioactivity peak was observed at elution volume 9–16 ml, corresponding to nanoparticle-associated radioactivity. This was followed by a small peak (equal to about 6% of the major peak) at elution volume 21–24 ml, corresponding to radioactivity probably dissociated from the nanoparticles during incubation. In the case of the nanoparticles pre-incubated in mice serum apart from these peaks, observed at the same elution volume as in the case of the control nanoparticles, a third peak was observed at elution volume 16–21 ml corresponding to the

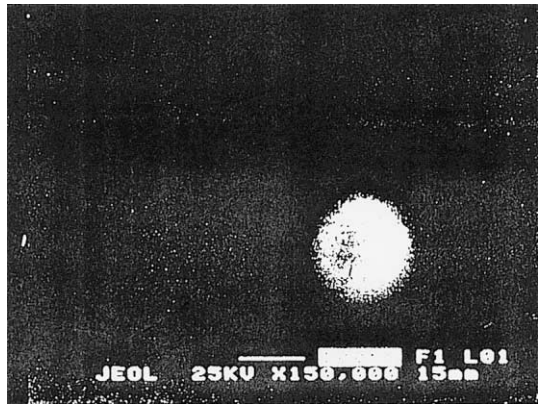

Fig. 1. Scanning electron micrograph of a PLGA(32)–mPEG(5) nanoparticle.

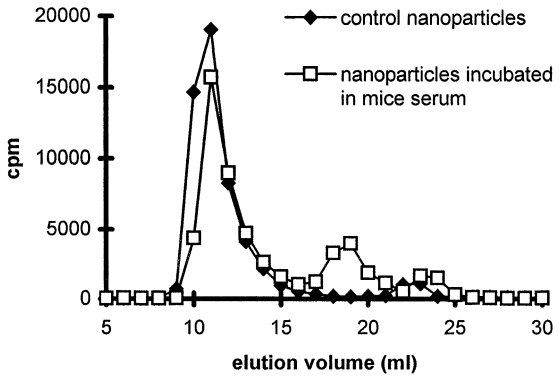

Fig. 2. Elution of ^{125}I-CA-labeled PLGA(32)–mPEG(5) nanoparticles from a Biogel A15m (1 × 45 cm) column after incubation in phosphate buffered saline (control nanoparticles) or in mice serum for 6 h at 37°C (eluent; phosphate buffered saline pH 7.4, flow rate; 4 ml/h).

elution of serum components, as control experiments with mice serum showed.

By comparing the radioactivity of the two major peaks (nanoparticle-associated radioactivity) it was found that the radioactivity remaining associated with the nanoparticles after 6 h incubation in mice serum at 37°C was about 80% of the radioactivity of the control nanoparticles incubated in PBS.

3.3. Effect of dose on the biodistribution and pharmacokinetics of PLGA and PLGA–mPEG nanoparticles

The variation of radioactivity level with time in blood, in MPS (liver and spleen) and in the remaining animal's tissues (carcass) following the i.v. administration of different doses of ^{125}I-CA-labeled PLGA and PLGA(32)–mPEG(5) nanoparticles is shown in Fig. 3. After the administration of the labeled nanoparticles, the radioactivity uptake into liver and spleen accounted consistently for the majority of the radioactivity uptake into MPS organs and, therefore, for the purposes of this study as MPS uptake was taken the uptake into liver and spleen. Irrespective of the administered dose, the radioactivity exhibited much higher blood circulation time in the case of PLGA–mPEG than in the case of PLGA nanoparticles (hours versus seconds). Also, for both types of nanoparticles and irrespective of dose, the level of radioactivity in carcass (animal's tissues other than the blood and MPS) was in the range of 20–30% of the dose throughout the time period studied (Fig. 3). The remainder 70–80% of the dose was distributed between blood and MPS indicating that the removal of the particles from blood with time was due to their capture in MPS.

In the case of the PLGA(32)–mPEG(5) nanoparticles, the radioactivity levels in blood and the uptake of radioactivity in MPS were not affected by the administered dose whereas in the case of PLGA nanoparticles they depended on dose (Fig. 3). The radioactivity level with time in different mice tissues is shown in Fig. 4 (only tissues with radioactivity higher than 1% of the dose were included). It appears that, for both nanoparticle types, the radioactivity levels in the other tissues (collectively referred to as carcass in this study) were not affected by the administered nanoparticle dose.

For both nanoparticle types, the blood data (radioactivity levels) obtained with the lowest dose at a specific time post-administration were compared with those obtained with the highest dose at the same post-administration time using two-sided t-tests (Statgraphics Plus 3.3 software). At all post-administration times, the effect of dose on the radioactivity levels in blood was significant ($P < 0.05$) in the case of PLGA nanoparticles and not significant ($P > 0.05$) in the case of the PLGA(32)–mPEG(5) nanoparticles.

Increasing the dose of the labeled PLGA nanoparticles caused an increase in blood residence and a decrease in MPS uptake of radioactivity (Fig. 3). The decrease in radioactivity MPS uptake with increasing the dose of the labeled PLGA nanoparticles resulted from a decrease in radioactivity capture in liver but not in spleen (irrespective of dose, radioactivity levels in spleen were 1–2% of the dose at all sampling times), indicating that a certain degree of liver saturation occurred at the higher doses of PLGA nanoparticles. Essentially, the dose of the labeled PLGA nanoparticles affected the radioactivity distribution between blood and liver but it did not affect the radioactivity levels in the other animal's tissues (Fig. 4).

After the i.v. administration of the ^{125}I-CA-labeled PLGA nanoparticles, the radioactivity followed non-linear pharmacokinetics whereas after the i.v. administration of the ^{125}I-CA-labeled and PLGA(32)–mPEG(5) nanoparticles the radioactivity followed linear pharmacokinetics (Fig. 5). In order to generate estimates of the basic pharmacokinetic parameters of both nanoparticle types, the radioactivity level in blood versus time data were analyzed according to a two compartment model in the case of PLGA nanoparticles and according to a one compartment model in the case of PLGA(32)–mPEG(5) nanoparticles. Regression analysis was applied in the blood data to

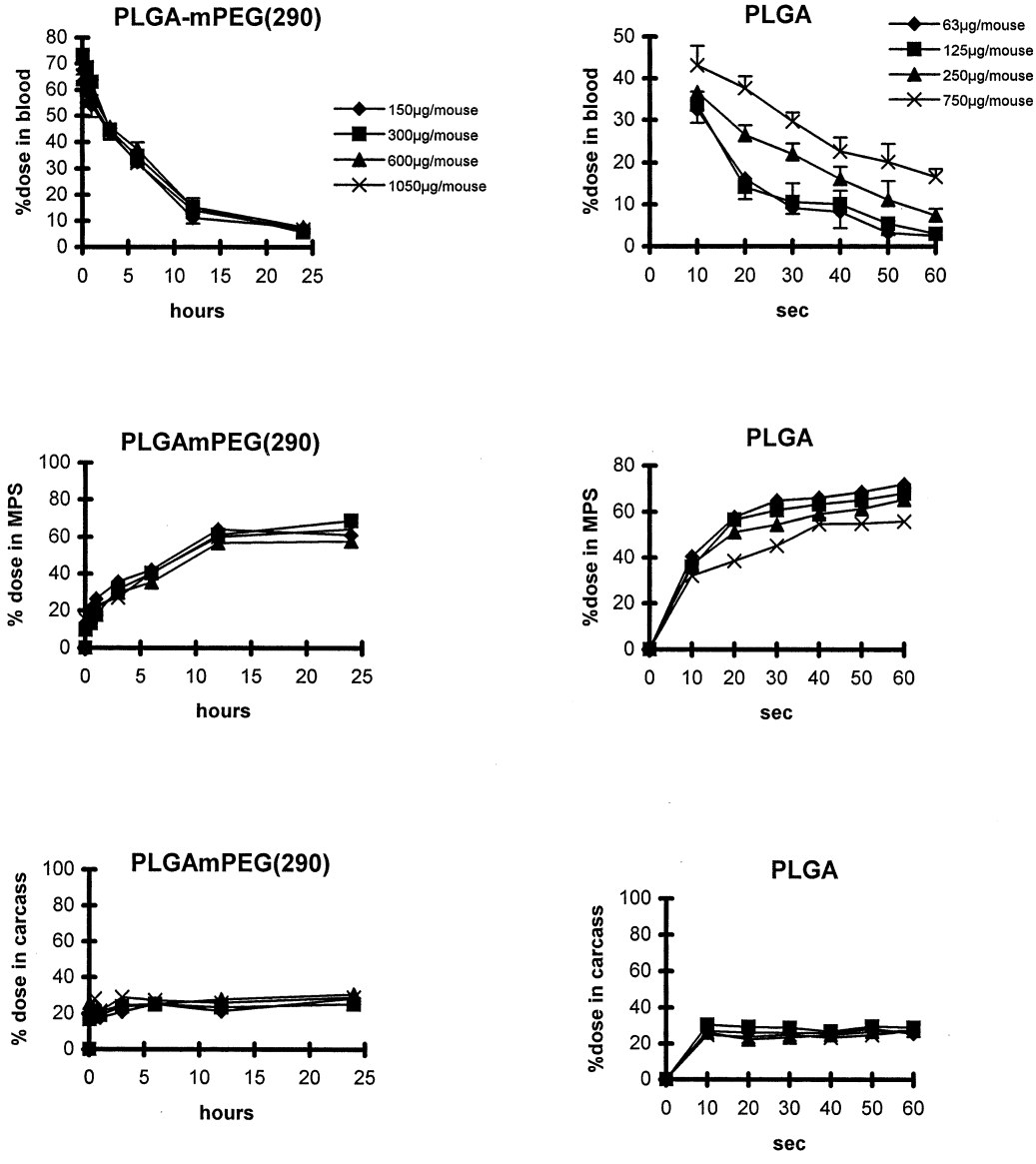

Fig. 3. Biodistribution of radioactivity with time in blood, MPS (liver and spleen) and carcass (all animal's tissues except blood and MPS) following the iv administration of different doses of ^{125}I-CA labeled PLGA and PLGA(32)–mPEG(5) nanoparticles in mice. Points and bars represent mean ($n = 3$) and standard deviation.

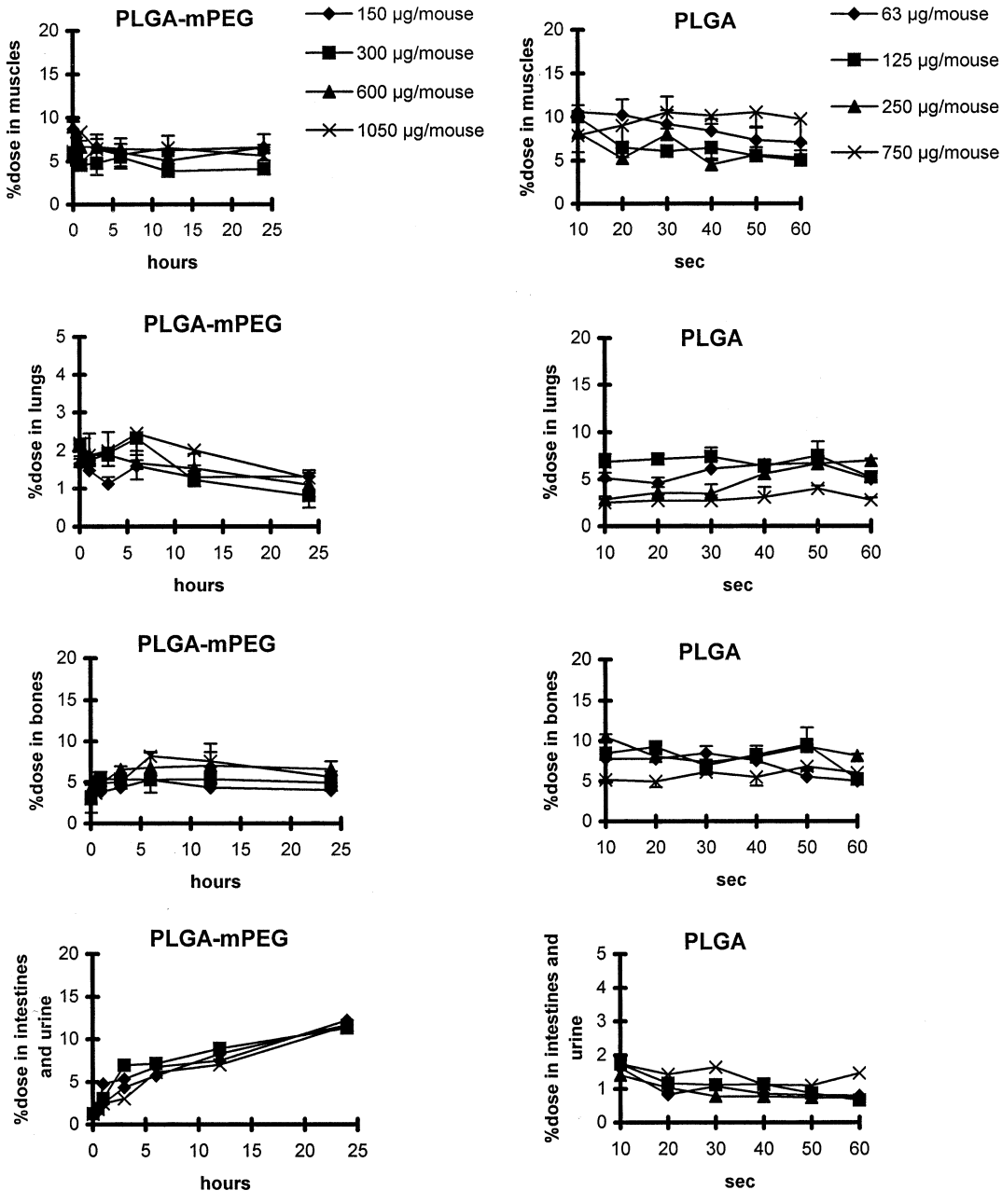

Fig. 4. Tissue distribution of radioactivity with time following the iv administration of different doses of ^{125}I-CA labeled PLGA and PLGA(32)–mPEG(5) nanoparticles in mice. Points and bars represent mean ($n = 3$) and standard deviation.

obtain elimination rate constants and biological half-lives. Then, well known pharmacokinetic functions (Gibaldi and Perrier, 1982) were applied in order to obtain the values of the rest parameters shown in Tables 1 and 2. For the PLGA nanoparticles, only the data of the central compartment (blood), which are the most important, are shown in Table 1 in order to facilitate their

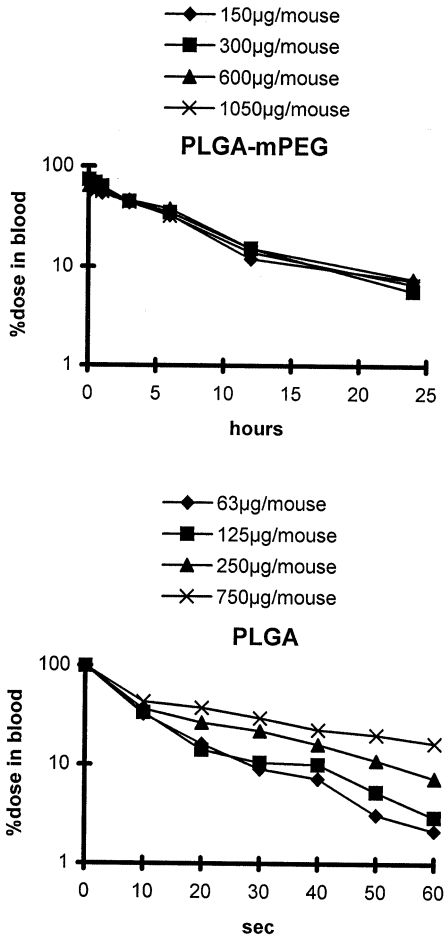

Fig. 5. Change of radioactivity level in blood with time (semi-logarithmic plot of mean values, $n = 3$) following the i.v. administration of different doses of ^{125}I-CA labeled PLGA and PLGA(32)–mPEG(5) nanoparticles in mice.

comparison with the same type of data obtained with the PLGA–mPEG nanoparticles. The half-life of the distribution phase for the PLGA nanoparticles could not be estimated due to their rapid removal from blood and it was not included in Table 1.

The data in Tables 1 and 2 indicate that the elimination rate constant (β or k_{el}), the biological half-life ($T^{\beta}_{1/2}$ or $T_{1/2}$) and the total body clearance depended on dose in the case of PLGA nanoparticles, whereas they were independent of dose in the case of PLGA(32)–mPEG(5) nanoparticles. There was a significant ($\sim$three-fold) increase in the biological half-life of the radioactivity with increasing dose of the labeled PLGA nanoparticles from 63 to 750 µg polymer per mouse, indicating that a certain degree of saturation of the mechanism of nanoparticle removal from blood (MPS uptake) occurred at higher nanoparticle doses.

The areas under the curve (AUC) increased with increasing dose for both nanoparticle types but were dramatically higher in the case of PLGA(32)–mPEG(5) nanoparticles (Tables 1 and 2). The latter becomes apparent when the AUC of both nanoparticle types is expressed in same units, e.g. if the areas are expressed in both cases in µg s/ml, then the AUC values in Table 2 should be multiplied by a factor of 3600 (1 h = 3600 s). The AUC increased disproportionately to increasing dose (about 25-fold AUC increase over a 12-fold dose increase) in the case of PLGA nanoparticles (Table 1) whereas it increased in proportion to the increasing dose (7-fold AUC increase over a 7-fold dose increase) in the case of and PLGA(32)–mPEG(5) nanoparticles (Table 2), additional evidence that the MPS uptake of PLGA, but not of PLGA–mPEG nanoparticles, becomes saturated as the nanoparticle dose increases.

Table 1
Pharmacokinetic parameters of PLGA nanoparticles derived using the mean ($n = 3$) nanoparticle levels in blood versus time data[a]

Dose (µg polymer per mouse)	β (s^{-1})	$T^{\beta}_{1/2}$ (s)	V_{β} (ml)	AUC (µg s/ml)	Body clearance (ml/s)
63	0.05	13.00	2.33	506.4	0.12
125	0.04	17.24	3.02	1029.8	0.12
250	0.03	22.50	2.45	3316.3	0.08
750	0.02	35.00	3.03	12 487.6	0.06

[a] $T^{\beta}_{1/2} = 0.693/\beta$, V_{β} = dose/β AUC, Body clearance = dose AUC, AUC = (area of trapezoids from $t = 0$ to 60 s) + ($C_{60\ s}/\beta$).

Table 2
Pharmacokinetic parameters of PLGA(32)–mPEG(5) nanoparticles derived using the mean ($n = 3$) nanoparticle levels in blood versus time data[a]

Dose (μg polymer per mouse)	k_{el} (h^{-1})	$T_{1/2}$ (h)	V_{darea} (ml)	AUC (μg h/ml)	Body clearance (ml/h)
150	0.10	7.08	1.79	845.5	0.18
300	0.11	6.45	1.52	1856.7	0.16
600	0.09	7.83	1.84	3618.5	0.16
1050	0.09	7.39	1.85	6040.2	0.17

[a] $T_{1/2} = 0.693/k_{el}$, $V_{darea} = \text{dose}/k_{el}$ AUC, Body clearance = dose AUC, AUC = (area of trapezoids from $t = 0$ to 24 h) + ($C_{24\ h}/k_{el}$).

4. Discussion

In this study, the effect of dose (μg polymer per mouse) on the biodistribution and pharmacokinetics of PLGA and PLGA–mPEG nanoparticles was investigated. The nanoparticles were labeled with ^{125}I-CA, administered i.v. in mice and the radioactivity levels in mice tissues at various times post-administration were measured. The stability of label association with the nanoparticles, as evaluated by the radioactivity loss from the nanoparticles after 6 h incubation with mice serum in vitro, was satisfactory (Fig. 2). The effect of nanoparticle dose was studied over an about 10-fold dose range. The selection of the dose range was based on calculations of the polymer doses (μg/kg) required for the delivery of therapeutic doses of relatively potent drugs, such as the anticancer drugs, even at low drug loading of 1–5% w/w.

Following their i.v. administration, both nanoparticle types were removed from systemic blood circulation through their capture in MPS. However, the rate this process took place was significantly different for the two nanoparticle types (Fig. 3). The PLGA nanoparticles were rapidly removed from blood, exhibiting biological half-lives in the range of 13–35 s for the doses applied in this study, whereas the PLGA–mPEG nanoparticles exhibited prolonged residence in blood with biological half-lives in the order of 7 h (Tables 1 and 2). The above values compare well with the values for the circulatory half-lives of the PLGA and PLGA–mPEG nanoparticles reported in the literature (Bazile et al., 1995). The rate of blood clearance and MPS uptake were found to depend on nanoparticle dose in the case of the PLGA nanoparticles whereas they were independent of dose (in the range of doses administered in the present study) in the case of the PLGA–mPEG nanoparticles (Figs. 3 and 5). Due to the significantly different blood removal rates of the two nanoparticle types, a different time period for blood sampling had to be applied for the two nanoparticle types in order to obtain a complete picture of their blood profile. Within the specific sampling time period used for each nanoparticle type, the PLGA nanoparticles followed non-linear and dose-dependent pharmacokinetics whereas the PLGA–mPEG nanoparticles followed linear and dose-independent pharmacokinetics (Fig. 5).

Increasing the nanoparticle dose caused a decrease in both the rate of blood clearance and the rate of MPS uptake of the PLGA nanoparticles (Figs. 3 and 5). Apparently, a decrease of MPS activity occurred with increasing doses of PLGA nanoparticles resulting either from the saturation of binding sites and uptake mechanisms or from the depletion of plasma opsonins (opsonization by plasma proteins, such as C3 complement protein (Artursson and Sjoholm, 1986), is considered to precede nanoparticle phagocytocis by macrophages). Whereas the dose affected the distribution of PLGA nanoparticles between blood and MPS (liver), it did not appear to affect the nanoparticle levels in the other mice tissues.

In conclusion, the nanoparticle dose appeared to affect significantly the biodistribution of the PLGA nanoparticles between blood and MPS but it did not appear to affect the biodistribution of the PLGA–mPEG nanoparticles in the range of doses applied here. The PLGA nanoparticles fol-

lowed non-linear and dose-dependent pharmacokinetics whereas the PLGA–mPEG nanoparticles followed linear and dose-independent pharmacokinetics, over a potential clinically relevant dose range applied in this study. In addition to the prolonged blood circulation time, the dosage-independence of the pharmacokinetics of the PLGA–mPEG nanoparticles provides further advantages for their application in controlled drug delivery and in drug targeting. Thus, the linear and dose-independent pharmacokinetics and the lack of MPS saturation observed with PLGA–mPEG nanoparticles simplify the selection of drug doses and dosing intervals and reduce the chances of MPS impairment when these nanoparticles are applied as drug carriers.

References

Allen, T.M., Stealth liposomes: avoiding reticuloendothelial uptake. G. Lopez-Berestein, I. Fidler (Eds.), Liposomes in the Therapy of Infectious Diseases and Cancer, UCLA Symposium on Molecular and Cellular Biology, Vol. 89, Alan R. Liss, New York, 1988, 405–415.

Artursson, P., Sjoholm, I., 1986. Effect of opsonins on the macrophage uptake of polyacrylstarch microparticles. Int. J. Pharm. 32, 165–170.

Bazile, D., Prud'Homme, C., Bassoullet, M.T., Marlard, M., Spenlehauer, G., Veillard, M., 1995. Stealth Me.PEG-PLA nanoparticles avoid uptake by the mononuclear phagocytes system. J. Pharm. Sci. 84, 493–498.

Beletsi, A., Leondiadis, L., Klepetsanis, P., Ithakissios, D.S., Avgoustakis, K., 1999. Effect of preparative variables on the properties of PLGA–mPEG copolymers related to their application in controlled drug delivery. Int. J. Pharm. 182, 187–197.

Chiotelis, E., Subramanian, G., McAfee, J.G., 1977. Preparation of Tc-99m labeled pyridoxal-amino acid complexes and their evaluation. Int. J. Nucl. Med. Biol. 4, 29–41.

Couvreur, P., Dubernet, C., Puisieux, F., 1995. Controlled drug delivery with nanoparticles: current possibilities and future trends. Eur. J. Pharm. Biopharm. 41, 2–13.

De Jaeghere, F., Allemann, E., Leroux, J.C., Stevels, W., Feijen, J., Doelker, E., Gurny, R., 1999. Formulation and lyoprotection of poly(lactic acid-co-ethylene oxide) nanoparticles: influence on physical stability and in vitro cell uptake. Pharm. Res. 16, 859–866.

Emile, C., Bazile, D., Herman, F., Helene, C., Veillard, M., 1996. Encapsulation of oligonucleotides in Stealth Me.PEG-PLA50 nanoparticles by complexation with structured oligopeptides. Drug Deliv. 3, 187–195.

Gibaldi, M., Perrier, D., 1982. Pharmacokinetics. Marcel Dekker, New York.

Gref, R., Minamitake, Y., Peracchia, M.T., Trubetskoy, V., Torchilin, V., Langer, R., 1994. Biodegradable long-circulating polymeric nanospheres. Science 263, 1600–1603.

Gref, R., Domb, A., Quellec, P., Blunk, T., Muller, R.H., Verbavatz, J.M., Langer, R., 1995. The controlled intravenous delivery of drugs using PEG-coated sterically stabilized nanospheres. Adv. Drug Deliv. Rev. 16, 215–223.

Kwon, G.S., 1998. Diblock copolymer nanoparticles for drug delivery. CRC. Crit. Rev. Ther. Drug Carrier Syst. 15, 481–512.

New, R.R.C., 1990. Liposomes: A Practical Approach. Oxford University Press, Oxford.

Peracchia, M.T., Gref, R., Minamitake, Y., Domb, A., Lotan, N., Langer, R., 1997. PEG-coated nanospheres from amphiphilic diblock and multiblock copolymers: Investigation of their drug encapsulation and release characteristics. J. Control. Release 46, 223–231.

Stolnik, S., Dunn, S.E., Garnett, M.C., Davies, M.C., Coombes, A.G.A., Taylor, D.C., Irving, M.P., Purkiss, S.C., Tadros, T.F., Davis, S.S., Illum, L., 1994. Surface modification of poly(lactide-co-glycolide) nanospheres by biodegradable poly(lactide)-poly(ethyleneglycol) copolymers. Pharm. Res. 11, 1800–1808.

Zambaux, M.F., Bonneaux, F., Gref, R., Dellacherie, E., Vigneron, C., 1999. MPEO-PLA nanoparticles: effect of MPEO content on some of their surface properties. J. Biomed. Mater. Res. 44, 109–115.